

**Characterization of  
glycosylphosphatidylinositol-anchored  
ceruloplasmin enriched in the apical plasma  
membrane of rat hepatocytes**

(ラット肝細胞のアピカル側細胞膜に局在する  
GPI-セルロプラスミンの特性に関する研究)

秋田大学大学院医学系研究科医学専攻  
分子機能学・代謝機能学講座  
(指導教授 杉山 俊博)

FLORES Maria Jolina Lou

**Characterization of glycosylphosphatidylinositol-anchored ceruloplasmin enriched in the apical plasma membrane of rat hepatocytes**

**Maria Jolina Lou N. Flores, Souichi Koyota, Zhiwei Qiao, Yukio Koizumi, and Toshihiro Sugiyama<sup>1</sup>**

*Department of Biochemistry, Akita University Graduate School of Medicine, 1-1-1 Hondo, Akita 010-8543, Japan*

Running title: GPI-Cp in apical plasma membrane of rat hepatocyte

<sup>1</sup>To whom correspondence should be addressed. Tel: +81 18-884-6074;  
Fax: +81 18-884-6443; E-mail: [sugiyama@med.akita-u.ac.jp](mailto:sugiyama@med.akita-u.ac.jp)

## **Abstract**

*Aim:* Ceruloplasmin (Cp) is an acute-phase protein and a member of the multicopper oxidase family of enzymes. It has been implicated in iron metabolism because of its ferroxidase activity. It is expressed as soluble (sCp) or glycosylphosphatidylinositol-anchored ceruloplasmin (GPI-Cp) form; the former is primarily synthesized in the liver, and the latter is primarily found in the brain. Although recent studies reported GPI-Cp expression on hepatocytes, little is known regarding its presence in specific liver cell compartments and its possible involvement in liver pathophysiology. This study aimed to characterize the distribution of GPI-Cp in liver cells and specifically in the apical part of the plasma membrane.

*Methods:* We assessed GPI-Cp expression in the liver using immunohistochemistry and immunoblotting techniques. Furthermore, we isolated apical and basolateral membrane fraction from the total liver membrane using sucrose discontinuous gradient centrifugation, and GPI-Cp were detected using immunoblotting.

*Results:* GPI-Cp was detected in purified apical membranes of rat liver cells. Immunoreactive Cp protein was released after incubation with phosphatidylinositol-specific phospholipase C, and the free protein demonstrated ferroxidase activity.

*Conclusion:* These findings suggest that majority of GPI-Cp present in the liver is primarily located on the apical surface of cells because of transcytosis.

**Key words:** apical membrane, ceruloplasmin, GPI-Cp, hepatocyte

## Introduction

Ceruloplasmin (Cp) was first isolated from blood plasma and characterized as a copper-containing protein by Holmberg and Laurell in 1948. It is an acute phase protein and a member of the multicopper oxidase family of enzymes, which contains more than 95% of the copper present in plasma<sup>1)</sup>. Cp, a major ferroxidase of plasma, is required for iron transport by transferrin. Oxidation of the ferrous iron Fe(II) to the ferric iron Fe(III) mediated by Cp is necessary for incorporation of iron into transferrin because transferrin binds only the ferric form of iron. As a ferroxidase, Cp may also play a role in the transferrin-independent iron uptake system, which requires reduction of iron on the cell surface<sup>2)</sup>. It is thought that in mammals, Cp is primarily synthesized as a soluble protein secreted by hepatocytes into plasma. On the other hand, GPI-Cp is predominantly expressed in astrocytes<sup>2)</sup>, leptomeningeal cells<sup>3)</sup>, retina<sup>4)</sup>, and testes<sup>5)</sup>. The recently revealed ubiquitous expression of the GPI-Cp in hepatocytes<sup>6-7)</sup> raises the question of its possible implication in liver pathophysiology.

Hepatocytes are major epithelial cells in the liver<sup>8)</sup>. A hepatocyte performs several crucial functions that are largely the result of its strategic position between 2 different environments: the blood plasma and the bile. Functions performed within both these domains are different, which means that the hepatocyte surface is asymmetric or polarized<sup>9)</sup>.

The plasma membrane of polarized epithelial cells is divided into 2 domains: apical (canalicular) and basolateral (sinusoidal)<sup>10)</sup>. Polarized cells have evolved various sorting mechanisms to supply their specialized membrane domains and the adjacent extracellular milieu with specific molecules<sup>11)</sup>. Therefore, a hepatocyte performs specialized functions<sup>10)</sup> such as canalicular bile secretion and simultaneous sinusoidal secretion of large quantities of serum proteins into the blood<sup>8)</sup>.

Glycosylphosphatidylinositol-anchored proteins (GPI-APs) are directly targeted to the apical domain of the plasma membrane in majority polarized epithelial cells<sup>10</sup>. Most GPI-APs in the liver follow the indirect pathway: first, they are transported to the basolateral surface, where they are internalized and redirected to the apical surface through transcytosis<sup>13-18</sup>.

In the present study, the previous observation that GPI-Cp is present in the rat liver was further explored using mRNA, immunohistochemical, and immunoblot assays. Furthermore, GPI-Cp distribution was analyzed within different domains of the plasma membrane of hepatocytes.

## **Materials and Methods**

### **Animals**

SD and LEC rats were kept in metabolic cages under controlled temperature conditions ( $23 \pm 2^\circ\text{C}$ ) in a 1:1 light–dark cycle (12 h/12 h). They had free access to distilled water and either CE-7 or CE-2 feed, respectively (CLEA Japan Inc., Japan). All studies were conducted in accordance with Akita University Animal Regulations.

### **Cell Culture**

Primary hepatocytes were isolated from rat livers using the 2-stage collagenase perfusion technique described previously<sup>19</sup>. C6 glioma cells were generously provided by the Department of Neurosurgery, Akita University Graduate School of Medicine, Japan.

### **Immunohistochemistry**

Cryostat sections of a 4% paraformaldehyde-fixed adult rat liver were immunohistochemically stained with a polyclonal goat anti-Cp (Sigma, USA), using a previously described protocol<sup>3</sup>. Visualization of the primary antibody was performed using a rabbit anti-goat IgG secondary antibody conjugated to biotin.

### **RNA extraction and RT-PCR**

Total RNA extraction was performed using RNAiso Plus (TAKARA Bio Inc., Japan), followed by quantitative and qualitative analysis. Briefly, to isolate RNA, cultured cells were washed and lysed in RNAiso Plus buffer. Thereafter, frozen liver and brain tissues were homogenized and lysed with RNAiso Plus. cDNA was synthesized with oligo(dT) primers according to the PrimeScript RT reagent Kit procedure (Takara Bio

Inc.). The resulting cDNA strand was used as a template for PCR with specifically designed primers as listed in Table 1. Subsequently, RT-PCR products were separated in 1.2% agarose gel (Takara Bio Inc.), stained with an ethidium bromide dropper bottle (CLP, USA), and photographed.

### **Isolation of the total liver plasma membrane**

The total liver plasma membrane (tLPM) was isolated as described previously<sup>20</sup>. Briefly, rats were ether-anesthetized and perfused through the portal vein with 50 mL isolation medium (0.25 M sucrose, 1 mM EGTA, and 5 mM K-HEPES; pH 7.4) at 37°C. The liver was then weighed, minced, washed twice with the same medium, and homogenized in 50 mL isolation medium by means of 10 passes using a loosely fitting pestle, followed by 3 passes using a tightly fitting pestle. The solution was diluted with the isolation medium to 6% (w/v) and then centrifuged for 10 min at 1,400 ×g. The resulting pellet was resuspended in the isolation medium to a final concentration of 6% and again homogenized in a tightly fitting pestle 4 times. Percoll was added to the suspension (1.4 mL Percoll per 10.4 mL suspension) and centrifuged for 30 min. The top fluffy layer (plasma membrane vesicles) was isolated, diluted to a concentration of 1:5 (v/v) with the incubation medium (0.25M sucrose and 50 mM Tris-HCl; pH 8.0) and centrifuged for 30 min at 34,500 ×g. Few isolated pellets (tLPM) were quickly frozen and stored until further experiments.

### **Isolation of apical and basolateral membrane fractions from the total liver plasma membrane**

We used a previously described method<sup>20</sup>, with minor modifications. The isolated tLPM was washed with 5 volumes of washing/incubation buffer (0.25M sucrose and

25 mM K-HEPES; pH 7.4) and sedimented for 5 min at 34,500 ×g to remove residual Percoll. TLPM was dissolved to attain a 5-mg/mL concentration with the same buffer and homogenized using 75 passes with a tightly fitting pestle. Thereafter, tLPM vesicles were layered on a discontinuous sucrose gradient (43%, 46%, and 52%) and centrifuged for 1 h at 93,000 ×g. The resulting pellet represents the basolateral plasma membrane (bLPM), which was then sedimented (10 min, 34,500 ×g) after addition of 5 volumes of the same buffer. On the other hand, apical LPM (aLPM) was carefully isolated from bands at the top of 43% and inside the 43%–46% sucrose interface, was resuspended in 5 volumes of the same buffer, and sedimented at 34,500 ×g for 10 min. Both aLPM and bLPM pellets were frozen and stored until further experiments. All procedures were conducted at 4°C, and solutions were prepared in the presence of 0.01% soybean trypsin inhibitor (STI) and 0.1 mM phenylmethanesulfonyl fluoride (PMSF)<sup>21</sup>.

## **Characterization of the plasma membrane of liver cells**

### ***Alkaline phosphatase activity***

Alkaline phosphatase activity was measured using the QuantiChrom Alkaline Phosphatase Assay Kit (BioAssay Systems, USA).

### ***Na/K-ATPase***

The Na/K-ATPase assay was performed using a previously described method<sup>22–25</sup>. An incubation medium containing (final concentrations) 100 mM NaCl, 20 mM KCl, 50 mM Tris-HCl (pH 7.2), 5 mM MgCl<sub>2</sub>, 2 mM Tris-ATP, with or without 7 mM ouabain, was preincubated at 37°C for 5 min. The reaction was initiated by adding 20 μL membrane suspension (0.5 mg protein/mL) to a 180-μL aliquot of the incubation medium. At the indicated time points, the reaction was stopped by addition of 300 μL



of ice-cold solution of 2.8% ascorbic acid, 0.48 M HCl, 0.48% ammonium molybdate, 2.8% SDS. After 10 min, 500  $\mu$ L of a solution containing 2% sodium arsenite, 2% sodium citrate, and 2% acetic acid was added and rewarmed to 37°C for 10 min, after which absorbance at 750 nm was measured. The Na/K-ATPase activity was calculated as the difference between the amount of inorganic phosphate liberated in the presence and absence of ouabain. The enzymatic activity was expressed as micromoles ( $\mu$ mol) of phosphate liberated per mg of protein per minute.

### ***5'-nucleotidase***

The 5'-nucleotidase activity was measured using a previously published protocol<sup>22</sup>. A reaction buffer containing (final concentrations) 90 mM Tris-HCl (pH 8.0), 10 mM MgCl<sub>2</sub>, 15 mg adenosine-5'-monophosphate along with membrane samples were incubated on a shaking water bath for 15 min. The reaction was stopped, by adding ice-cold TCA (final concentration, 30%); thereafter, the mixture was incubated with 10% ascorbic acid and 0.42% ammonium molybdate, and absorbance at 750 nm was measured. The 5'-nucleotidase activity was calculated as the released phosphate in each sample tube using the standard curve and was expressed as micromoles ( $\mu$ mol) of phosphate per mL per hour.

### ***Protein assay***

Protein concentrations were measured using the BCA Protein Assay Kit (Thermo Scientific, USA).

### **PI-PLC treatment of membrane fractions**

Following previously described protocols<sup>5,26</sup>, plasma membrane fractions and microdomains (200  $\mu$ g protein) were incubated with or without phosphatidylinositol-

specific phospholipase C (PI-PLC; 0.5 U/mL; Molecular Probes, USA) containing a protease inhibitor cocktail (PIC; 20  $\mu$ L/mL; Sigma-Aldrich, USA) and PMSF (200  $\mu$ M) for 1 h at 37°C with shaking. The suspension was again centrifuged (15,700  $\times g$ , 30 min, 4°C), and the plasma membrane in the supernatant containing the released Cp was precipitated, by adding ice-cold TCA (final concentration, 10%). The mixture was left on ice for 30 min and then centrifuged (11,300  $\times g$ , 20 min, 4°C). Protein pellets were resuspended in PBS to a protein concentration.

### **Immunoblotting**

Proteins were separated by means of gel electrophoresis on 7%–10% gels and then transferred onto PVDF membranes according to published protocols<sup>2,5</sup>. All blots were blocked with 5% skim milk in Tris-buffered saline containing 0.1% Tween 20 (TBS-T buffer) for 1 h. For detection of Cp, all blots were incubated with a goat antihuman Cp antibody (1:1,000 in blocking buffer; Sigma-Aldrich) for 1 h at room temperature or overnight at 4°C. Thereafter, blots were incubated with a biotinylated rabbit antigoat IgG antibody (1:10,000 in blocking buffer; Sigma-Aldrich, USA) for 45 min at room temperature and with horseradish peroxidase-conjugated avidin (Vectastain elite ABC Kit; Vector laboratories, USA) for 30 min at room temperature. All blots were washed between incubations with TBS-T and were visualized using enhanced chemiluminescence (ECL; Amersham, GE Healthcare, UK).

### **Triton X-114 extraction and phase partitioning**

The procedure for Triton-X114 (TX-114) extraction and phase partitioning has been described earlier<sup>5,26</sup>. Plasma membrane fractions (200  $\mu$ g protein) were precipitated by adding ice-cold TCA (final concentration, 10%) and allowed to stand on ice for 30 min and centrifuged thereafter (11,300  $\times g$ , 20 min, at 4°C). Pellets were resuspended

in 0.17 mL PBS (pH 7.4), with or without PI-PLC (5.4 U/mL). Reaction mixtures contained a protease inhibitor cocktail (PIC; 20  $\mu$ L/mL; Sigma-Aldrich) and PMSF (200  $\mu$ M) and were incubated for 80 min at 37°C. To the suspension, we added 1/5<sup>th</sup> volume of ice-cold precondensed TX-114; the mixture was then left on ice for 25 min with occasional agitation. After centrifugation (10,000  $\times$ g, 10 min at 4°C), undissolved material was removed and prepared for electrophoresis. Supernatants were prepared for separation into detergent and aqueous phases by heating to 37°C and centrifugation (1,000  $\times$ g, 10 min). Each phase was then collected and prepared for electrophoresis.

### **Detection of ferroxidase activity**

Ferroxidase activity was measured as described previously<sup>2)</sup>. Briefly, plasma membrane fractions (200  $\mu$ g protein) were precipitated by adding ice-cold TCA (final concentration, 10%), allowed to stand on ice for 30 min, and was then centrifuged (11,300  $\times$ g, 20 min at 4°C). Pellets were resuspended in 1 $\times$  PBS (pH 7.4), with or without PI-PLC (0.5 U/mL) and incubated for 60 min at 37°C. Thereafter, supernatants were concentrated using Amicon Ultra-0.5 Centrifugal Filter Devices (Millipore, Ireland) and separated by means of nondenaturing polyacrylamide gel electrophoresis using the Laemmli buffer system without SDS. Gels were incubated in 0.1 M sodium acetate (pH 5.7) containing 1 mg/mL *p*-phenylenediamine, which yields a purple precipitate upon oxidation.

### **Statistical Analysis**

Data were calculated as mean  $\pm$  SEM using Microsoft Office Excel. Student's unpaired 2-tailed *t* test was used for comparison of data between both membrane fractions.

## Results

### **GPI-anchored Cp expression on the surface of rat liver cells**

Most GPI-anchored proteins can be released from the cell surface by the bacterial enzyme PI-PLC<sup>5)</sup>. To detect Cp in the membrane surface from the rat liver, which corresponds to the GPI-Cp isoform, tissue samples were treated with PI-PLC prior to Cp immunostaining. Control tissue samples revealed stronger cell surface staining for Cp (Fig. 1A). In contrast, PI-PLC-treated tissue demonstrated a marked reduction in Cp staining (Fig. 1C).

Furthermore, we analyzed mRNA expression of sCp and GPI-Cp of both cells and tissues of the liver and brain using appropriate primers with RT-PCR. The full-length cDNA of rat GPI-Cp has been previously isolated from rat C6 glioma cells<sup>3)</sup>, which were cells representing the brain. As presented in Figure 2A and B, successful amplification of both sCp and GPI-Cp mRNA was accomplished in both liver and brain samples. However, as expected, mRNA expression of sCp in hepatocytes and liver tissue was greater compared with that in the GPI-Cp fraction, whereas C6 glioma cells and brain tissue revealed negligible sCp expression compared with that in the GPI-Cp fraction.

Another method that we used to confirm the presence of GPI-Cp in the liver was analysis of protein expression using immunoblotting. The membrane fraction was probed with a polyclonal goat antihuman Cp antibody and revealed a band with an apparent molecular weight of 148-kDa (Fig. 3). To evaluate whether the Cp protein detected was GPI-anchored, few membrane samples were treated with PI-PLC and separated into the released supernatant and the membrane pellet fraction. The PI-PLC-treated membrane pellet fraction appeared to contain less immunoreactive Cp compared with the PI-PLC-untreated membrane fraction. In addition, treated

supernatant fractions revealed greater concentrations of released GPI-Cp compared with PI-PLC-untreated supernatants. All these findings suggest that Cp present in the plasma membrane fraction of rat liver cells corresponds to the GPI-anchored form.

### **Detection of GPI-Cp in aLPM and bLPM**

Moreover, we evaluated Cp protein expression in rat liver membrane fractions. To separate tLPM into apical and basolateral domains, additional fractionation was performed using discontinuous sucrose gradient centrifugation<sup>15)</sup>. Both membrane domains of liver cells were assessed for purity using specific assays for alkaline phosphatase and 5'-nucleotidase as apical markers<sup>20,22)</sup>, along with an assay for Na/K-ATPase as a basolateral marker<sup>20,23-25)</sup>. As presented in Table 2, aLPM was enriched 2- and 27-fold compared with bLPM, as measured by 5'-nucleotidase and alkaline phosphatase assays, respectively. In contrast, bLPM was enriched by more than 4-fold over aLPM, according to Na/K-ATPase activity.

Further, we used immunoblotting to determine whether GPI-Cp is attached to the membrane through the GPI anchor. As presented in Figure 4, membrane-bound Cp was preferentially localized in aLPM of the plasma membrane. A significant difference was evident in the presence of membrane-bound Cp (GPI-Cp) between membrane domains (Fig. 4B,  $p < 0.001$ ). Furthermore, when both membranes were incubated with PI-PLC, aLPM supernatant fractions revealed higher concentrations of released GPI-Cp compared with untreated ones, whereas treated aLPM pellets revealed lower immunoreactive Cp signals (Fig. 5). Moreover, significant relevant bands were not detected in the basolateral membrane fraction. These results suggest that the GPI-anchored Cp was preferentially localized to the apical domain of the plasma membrane of liver cells.

### **Cp in membrane domains was covalently attached to GPI**

To confirm that Cp expressed in membrane fractions was covalently linked to GPI, immunoblotting of TX-114-treated samples was performed. Here equal protein concentrations of tLPM, aLPM, and bLPM were preincubated with or without PI-PLC and then solubilized using TX-114. Thereafter, samples were partitioned into aqueous and detergent phases. All Cp from untreated membrane fractions primarily partitioned into the detergent phase (Figs. 6A and B) because the GPI-anchored protein (containing an intact GPI anchor) partitioned into the detergent phase after TX-114 extraction because of the presence of hydrophobic lipid chains on the GPI anchor<sup>5</sup>).

PI-PLC digestion removes GPI-anchored proteins from the hydrophobic portions of the GPI anchor and causes these proteins to partition into the aqueous phase; these results support our data showing that PI-PLC-treated membranes exhibited higher Cp concentrations in the aqueous phase (Figs. 6C and D). These findings confirmed that Cp is directly anchored to the liver cell membrane by GPI rather than through association with some other GPI-anchored proteins<sup>5</sup>).

### **Oxidase activity of GPI-Cp**

To determine whether GPI-Cp found in liver cell membranes has a functional oxidase activity, tLPM, aLPM, and bLPM fractions were incubated with PI-PLC, and resulting supernatants were analyzed using native PAGE. Gels were then stained with *p*-phenylenediamine, which produces a purple precipitate when oxidized. The same procedure was performed with control samples, except for the PI-PLC treatment. Both PI-PLC-treated and PI-PLC-untreated tLPM and aLPM fractions revealed a band slightly lower than the Cp control (Fig. 7).

### **Increased GPI-Cp expression during copper accumulation**

Figure 8 shows increased GPI-Cp presence in liver cell membranes from LEC rats. LEC rat plasma membranes showed no specific localization of GPI-Cp between both membrane domains, in contrast to the apical preference of the normal SD membrane samples (Fig. 8A). In addition, the same 148-kDa band was present in LEC rat cellular membranes, although the amount of this protein was almost identical in aLPM and bLPM fractions. Furthermore, treatment of LEC membranes with PI-PLC allowed us to confirm that the attachment of Cp to both aLPM and bLPM occurs through its GPI anchor, after we observed a robust signal in the supernatant corresponding to the released GPI-Cp (Fig. 8B). Band signals of LEC rats were stronger compared with those of GPI-Cp bands from healthy SD rats. After PI-PLC treatment, supernatant fractions of LEC rats revealed higher immunoreactive Cp compared with corresponding pellet fractions, although LEC rat membranes still demonstrated higher Cp concentrations compared with those in membranes from samples from SD rats (Fig. 8C).

On the basis of above findings, it was evident that detected GPI-Cp bands in membrane fractions from LEC rats were more intense compared with membranes from healthy rats; however, differences between aLPM and bLPM were indiscernible.

## Discussion

A previous report<sup>27)</sup> indicated the presence of GPI-Cp in the liver in addition to its significant transcriptional expression in HepG2 cells. Since then, it has been proven that even at the protein level, hepatocytes express the GPI-Cp isoform in addition to the secreted form of Cp<sup>6,7)</sup>. Nevertheless, knowledge regarding GPI-Cp in the liver is still limited. We now confirmed the presence of GPI-Cp at both mRNA and protein levels in the rat liver.

In fact, GPI-Cp localization in the liver was demonstrated here by following results: (i) tissue-surface staining was markedly decreased after treatment with PI-PLC; (ii) the presence of mRNA corresponding to GPI-Cp was detected using RT-PCR; and (iii) Western blot analysis demonstrated that PI-PLC-treated membranes released a 148-kDa band that was immunoprecipitated by a polyclonal anti-Cp antibody. The treatment of whole cells or membrane preparations with PI-PLC has become a standard test for the presence of GPI-anchored proteins (GPI-APs). Therefore, the 148-kDa band detected in the liver membrane after PI-PLC treatment confirms the presence of GPI-Cp in the plasma membrane of liver cells.

In this report, we further analyzed the sorting of GPI-Cp between apical and basolateral domains of liver cells. We wished to determine whether GPI-Cp follows the typical transport route of GPI-APs in the liver, and whether the end point of GPI-Cp in the liver is linked to ferroxidase activity. It is widely accepted that GPI-APs are directly targeted to the apical domain of the plasma membrane in majority polarized epithelial cells<sup>14,15)</sup>. Our results support the existence of GPI-Cp in both apical and basolateral parts of the plasma membrane; however, this protein is significantly more abundant on the apical surface. This phenomenon could be interpreted in 2 ways: (a) GPI-Cp is expressed in both apical and basolateral domains, but most of it is sorted to



the apical side and (b) GPI-Cp, like other GPI-APs, follows the transcytosis pathway during protein sorting. The evidence that GPI-Cp has ferroxidase activity in the apical but not the basolateral membrane supports the second possibility.

In addition, it was hypothesized that the presence of GPI-Cp in the brain, kidney, and retina corresponds to blood–tissue barrier for iron trafficking<sup>7)</sup>. Therefore, in the liver, an array of tight junction molecules line bile canaliculi, thereby forming the blood–biliary barrier<sup>29,30)</sup>. On the other hand, the presence of GPI-CP with ferroxidase activity in the apical membrane seems to be a novel finding, in line with the existing knowledge that Cp performs a majority of the ferroxidase activity in the liver<sup>1–7)</sup>. Nonetheless, convincing evidence of the role of GPI-Cp in iron metabolism, particularly on the apical side, is yet to be elucidated.

Another significant finding in this work is the increased protein expression of GPI-Cp in the liver of LEC rats, which serves as an experimental model of hepatitis and Wilson’s disease. Cp has been known to be an acute-phase glycoprotein, whose gene has an IL-6 response element, and whose levels increase in blood in response to infection, inflammation, or trauma<sup>31–33)</sup>. To the best of our knowledge, there is no data on GPI-Cp levels under these pathological conditions. Nevertheless, previous studies have reported increased GPI-Cp protein levels following copper accumulation<sup>7)</sup>. Because LEC rats form an appropriate animal model of Wilson’s disease<sup>34,35)</sup>, which involves accumulation of copper in some tissues<sup>36,37)</sup>, GPI-Cp overexpression is an expected finding in LEC rats.

In conclusion, our findings extend previously reported data on localization of not only secretory Cp but also the membrane form of Cp (GPI-Cp) in the liver<sup>6,7)</sup>. Moreover, we were able to further pinpoint the location of GPI-Cp, which turned out to be the apical membrane of liver cells. The apical membrane has short transit on the

basolateral side, suggesting that GPI-Cp, like other GPI-APs, follows the indirect or transcytosis pathway during protein sorting. More detailed research into its possible relevance to copper and iron metabolism in the liver is a subject of an upcoming project.

## References

1. Hellman, N. and Gitlin, J. (2002) Ceruloplasmin metabolism and function. *Annu. Rev. Nutr.*, 22, 439-458.
2. Patel, B. and David, S. (1997) A novel glycosylphosphatidylinositol-anchored form of ceruloplasmin is expressed by mammalian astrocytes. *J. Biol. Chem.*, 272, 20185-20190.
3. Mittal, B., Doroudchi, M, Jeong SY, Patel B, David S. (2003) Expression of a membrane-bound form of the ferroxidase ceruloplasmin by leptomeningeal cells. *Glia*, 41, 337-346.
4. Chen, L, Dentchev, T., Wong, R., Wen, R., Bennett, J. and Dunaief, J.L. (2003) Increased expression of ceruloplasmin in the retina following photic injury. *Mol. Vis.*, 9, 151-158.
5. Fortna, R., Watson, H. and Nyquist, S. (1999) Glycosylphosphatidylinositol-anchored ceruloplasmin is expressed by rat sertoli cells and is concentrated in detergent-insoluble membrane fractions. *Biol of Repro.*, 61, 1042-1049.
6. Marques, L., Auriac, A., Willemetz, A., Banha, J., Silva, B., Canonne-Hergaux, F. and Costa, L. (2012) Immune cells and hepatocytes express glycosylphosphatidylinositol- anchored ceruloplasmin at their cell surface. *Blood Cells, Molecules, and Diseases*, 48, 110-120.
7. Mostad, E. and Prohaska, J. (2011) Glycosylphosphatidylinositol-linked ceruloplasmin is expressed in multiple rodent organs and is lower following dietary copper deficiency. *Exp Biol Med.*, 236, 298-308.
8. Wang, L., and Boyer, J. (2004) The maintenance and generation of membrane polarity in hepatocytes. *Hepatology*, 39, 892-899.
9. Arias, I., Alter, H., Boyer, J., Cohen, D., Fausto, N., Shafritz, D. and Wolkoff, A. (2009) Hepatocyte Surface Polarity: Its Dynamic Maintenance and Establishment. In: *The liver Biology and Pathobiology* (5<sup>th</sup> edition). UK: Wiley-Blackwell Publishing, 73-105.
10. Paladino, S., Sarnataro, D., Pillich, R., Tivodar, S., Nitsch, L. and Zurzolo, C. (2004) Protein oligomerization modulates raft partitioning and apical sorting of GPI-anchored proteins. *J Cell Biol.*, 167, 699-709.
11. Vuong, T.T., Prydz, K. and Tveit, H. (2006) Differences in the apical and basolateral pathways for glycosaminoglycan biosynthesis in madin-darby canine kidney cells. *Glycobiology*, 16, 326-332.
12. Decaens, C., Durand, M., Grosse, B. and Cassio, D. (2008) Which in vitro models could be best used to study hepatocyte polarity? *Biol. Cell*, 100, 387-398.

13. Nelson, W.J. and Rodriguez-Boulan, E. (2004) Unravelling protein sorting. *Nat. Cell Biol.*, 6, 282-284.
14. Paladino, S., Lebreton, S., Tivodar, S., Campana, V., Tempere, R. and Zurzolo, C. (2008) Different GPI-attachment signals affect the oligomerisation of GPI-anchored protein and their apical sorting. *J. Cell Sci.*, 21, 4001-4007
15. Weisz, O. and Rodriguez-Boulan, E., (2009) Apical trafficking in epithelial cells: signals, clusters and motors. *J. Cell Sci.*, 122, 4253-4266.
16. Treyer, A. and Musch, A. (2013) Hepatocyte Polarity. *Compr Physiol.*, 3, 243-287
17. Slimane, T., Trugnan, G., Van IJzendoorn, S. and Hoekstra, D. (2003) Raft-mediated trafficking of Apical Resident Proteins Occurs in Both Direct and Transcytotic Pathways in Polarized Hepatic Cells: Role of Distinct Lipid Microdomains. *Mol. Biol. Cell.*, 14, 611-624
18. Paladino, S., Pocard, T., Catino, M.A. and Zurzulo, C. (2006) GPI-anchored proteins are directly targeted to the apical surface in fully polarized MDCK cells. *J. Cell. Biol.*, 172, 1023-1035.
19. Berry, M. and Friend, D. (1969) High-yield preparation of isolated rat liver parenchymal cells. *J. Cell. Biol.*, 43, 506-520.
20. Cefaratti, C., Romani, A. and Scarpa, A. (2000) Differential localization and operation of distinct Mg<sup>2+</sup> transporters in apical and basolateral sides of rat liver plasma membrane. *J. Biol. Chem.*, 275, 3772-3780.
21. Tietz, P., Holma, R., Miller, L. and LaRusso, N. (1995) Isolation and characterization of rat cholangiocyte vesicles enriched in apical or basolateral plasma membrane domains. *Biochem.*, 34, 15436-15443.
22. Tuma, P. L. and Hubbard, A. L. (2001) Isolation of Rat Hepatocyte Plasma Membrane Sheets and Plasma Membrane Domains. In: *Current Protocols in Cell Biology* (1<sup>st</sup> edition). 2:3.2.1–3.2.16.
23. Proverbio, F., Proverbio, T. and Marin, R. (1986) Na<sup>+</sup>-ATPase in rat kidney basolateral plasma membranes. *Biochim. Biophys. Acta.*, 858, 202-205.
24. Marin R., Proverbio, T. and Proverbio, F. (1986) Inside-out basolateral plasma membrane vesicles from rat kidney proximal tubular cells. *Biochim. Biophys. Acta.*, 858: 195-201.
25. Reyes, A., Galindo, M.M., Garcia, L., Segura-Pena, D., Caruso-Neves, C., Eblen-Zajjur, A., Proverbio, T., Marin, R. and Proverbio, F. (2009) Ouabain-insensitive, Na<sup>+</sup>-stimulated ATPase of several rat Tissues: Activity during a 24h period. *Physiol. Res.*, 58, 693-699.

26. Ali, N. and Evans, W.H. (1990) Priority targeting of glycosylphosphatidylinositol-anchored proteins to the bile-canalicular plasma membrane of the hepatocytes. *Biochem. J.*, 271, 193-199.
27. Banha, J., Marques, L., Oliveira, R., Martins, M.F., Paixao, E., Pereira, D., Malho, R., Penque, D. and Costa, L. (2008) Ceruloplasmin expression by human peripheral blood lymphocytes: A new link between immunity and iron metabolism. *Free Radic. Biol. Med.*, 44, 483-492.
28. Ferguson, M. (1999) The structure, biosynthesis and functions of glycosylphosphatidylinositol anchors, and the contributions of trypanosome research. *J. Cell Sci.*, 112, 2799-2809.
29. Lee, N. and Luk, J. (2010) Hepatic Junctions: From viral entry to cancer metastasis. *World J. Gastroenterol.*, 16: 285-295.
30. Kojima, T., Yamamoto, T., Murata, M., Chiba, H., Kokai, Y. and Sawada N. (2003) Regulation of the blood-biliary barrier: interaction between gap and tight junctions in hepatocytes. *Med. Electron Microsc.*, 36, 157-164.
31. Aldred, A., Grimes, A., Schreiber, G. and Mercer, J. (1987) Rat Ceruloplasmin. Molecular Cloning and gene expression in liver, choroid plexus, yolk sac, placenta, and testes. *J. Biol. Chem.*, 262, 2875-2878.
32. Wiggins, J., Goyal, M., Wharram, B. and Wiggin, R. (2006) Antioxidant ceruloplasmin is expressed by glomerular parietal epithelial cells and secreted into urine in association with glomerular aging and high calorie diet. *J. Am. Soc. Nephrol.*, 17, 1382-1387.
33. Gitlin, J.D. (1988) Transcriptional regulation of ceruloplasmin by IL6 response element pathway. *J. Biol. Chem.*, 263, 6281-6287.
34. Kodama, H., Murata, Y., Mochizuki, D. and Abe, T. (1998) Copper and ceruloplasmin metabolism in the LEC rat, an animal model for Wilson disease. *J. Inher. Metab. Dis.*, 21, 203-206.
35. Wu, J., Forbes, J.R., Chen, H.S. and Cox, D.W. (1993) The LEC rat has a deletion in the copper transporting ATPase homologous to the Wilson disease gene. *Nature Genetics.*, 7, 541-545.
36. Li, Y., Togashi, Y., Sato, S., Emoto, T., Kang, J.H., Takeichi, N., Kobayashi, H., Kojima, Y., Une, Y. and Uchino, J. (1991) Spontaneous hepatic copper accumulation in Long-Evans Cinnamon rats with hereditary hepatitis. *J. Clin. Invest.*, 87, 1858-1861.
37. Li, Y., Togashi, Y., Sato, S., Emoto, T., Kang, J.H., Takeichi, N., Kobayashi, H., Kojima, Y., Une, Y. and Uchino, J. (1991) Abnormal copper accumulation in non-cancerous and cancerous liver tissues of LEC rats developing hereditary hepatitis and spontaneous hepatoma. *Jpn. J. Cancer Res.*, 82, 490-492.

## Figure Legends

**Fig. 1.** Immunohistochemistry images of rat liver tissue. Tissues were treated or not treated with PI-PLC. (A) Cp immunofluorescent staining of untreated tissue was markedly increased. (C) When rat liver tissue was treated with PI-PLC, Cp immunofluorescent staining was markedly decreased. (B, D) DAPI staining of cell nuclei of images in A and C, respectively.

**Fig. 2.** mRNA expression of sCp and GPI-Cp in the rat liver. (A) mRNA expression of the 2 forms of ceruloplasmin: soluble-Cp and GPI-Cp. Representative liver samples: liver tissue homogenates (lane 1) and hepatocytes (lane 2); brain samples: brain tissue homogenates (lane 3) and C6 glioma cells (lane 4). (B) Relative mRNA levels of sCp and GPI-Cp. Data are shown as mean  $\pm$  SEM. Loading amounts ( $\mu$ g) were equal for all samples.

**Fig. 3.** Detection of the 148-kD Cp protein in tLPM released by PI-PLC digestion. TLPM fractions were incubated with PI-PLC to release GPI-anchored proteins and eventually separated into the supernatant and pellet. Rat Cp was used as a positive control.

**Fig. 4.** Detection of the 148-kD Cp protein in aLPM. (A) Detection of preferential apical localization of a 148-kD protein band in the liver. (B) Relative intensity of Cp expression is significantly greater in aLPM compared with bLPM.  $*P < 0.001$ , Student's *t* test.

**Fig. 5.** Immunoblotting detection of a 148-kD GPI-anchored protein by an anti-Cp polyclonal antibody in aLPM and bLPM. Membrane fraction domains were incubated with PI-PLC to release GPI-anchored proteins and were eventually separated into the supernatant and pellet. Rat Cp was used as a positive control.

**Fig. 6.** Phase partitioning of GPI-Cp in TX-114 liver membrane fractions. Three membrane fractions were each subjected to either: (A) a mock incubation or (C) PI-PLC treatment to release the Cp proteins from the hydrophobic portion of its GPI anchor. After extraction with TX-114 and partitioning of detergent and aqueous phases, same as before, proteins were separated using SDS-PAGE, transferred to a PVDF membrane, and probed with an anti-Cp polyclonal antibody. Rat Cp was used as a positive control. (B, D) Relative intensity of Cp protein expression in untreated and PI-PLC-treated membrane samples, respectively.

**Fig. 7.** Ferroxidase activity of GPI-Cp in tLPM and aLPM. GPI-anchored proteins, released from liver membranes by PI-PLC treatment, were subjected to native PAGE, and the gel was stained with *p*-phenylenediamine to reveal the presence or absence of oxidase activity. In tLPM and aLPM, both whole membrane samples (lane 1) and the PI-PLC treated supernatant (lane 2) demonstrated ferroxidase activity.

**Fig. 8.** Increased Cp expression in liver cell membranes of LEC rats. (A) Detection of a robust 148-kD band in LEC rats compared with (control) SD rats. Cellular membranes of LEC rats revealed no significant difference in localization in tLPM, aLPM and bLPM, in contrast to the preference for aLPM in healthy rats. (B, C) Detection of a 148-kDa GPI-anchored protein by an anti-Cp polyclonal antibody in

both normal and LEC membrane samples. Membrane fractions of different domains were incubated with PI-PLC to release GPI-anchored proteins and eventually separated into the supernatant (B) and pellet (C). Thereafter, experimental samples were separated using SDS-PAGE, transferred to a PVDF membrane, and probed with a polyclonal antibody to human Cp. Rat Cp was used as a positive control.



**Table 1** PCR primers and conditions used in this study

	<b>Sequence (5'-3')</b>	<b>PCR product length (bp)</b>	<b>PCR conditions</b>
Rat-Cp	GGCCACAGCTTCCAATACAAG AGAGTCCTTTCAGTGCAGGTG	386	33 cycles 94°C ,2 min; 94°C, 30s, 55°C, 30 s; 72°C, 0.4s
GPI-Cp	GTATGTGATGGCTATGGGCAATGA CCTGGATGGAAGTGGTGATGGA	427	33 cycles 94°C ,2 min; 94°C, 30s, 55°C, 30 s; 72°C, 0.4s
B-actin	CTGAGGAGCACCTGTGCTG GGCATGAGGGAGCGCGTAAC	229	23 cycles 94°C ,2 min; 94°C, 30s, 55°C, 30 s; 72°C, 0.4s

**Table 2** Enzyme activity of purified apical and basolateral liver plasma membranes

	<u>Alkaline phosphatase</u> ( $\mu\text{mol}/\text{L}\times\text{min}$ )	<u>Na/K-ATPase</u> ( $\text{nmol}/(\text{mg}\times\text{min})$ )	<u>5-Nucleotidase</u> ( $\mu\text{mol}/(\text{mL}\times\text{h})$ )
tLPM	$3.6 \pm 1.74$	$30.8 \pm 4.6$	$14.07 \pm 2.19$
aLPM	$7.83 \pm 5.94$	$4.6 \pm 2.3$	$14.03 \pm 2.16$
bLPM	$-0.29 \pm 0.8$	$20.2 \pm 5.6$	$5.64 \pm 3.12$

Alkaline phosphatase activity is expressed in  $\mu\text{mol}/(\text{L}\times\text{min})$ , 5'-nucleotidase in  $\mu\text{mol}/(\text{mL}\times\text{h})$ , and Na/K-ATPase activity is expressed in  $\text{nmol}/(\text{mg}\times\text{min})$ . All data are presented as mean  $\pm$  SEM; n = 2 for all assays.

Figure 1

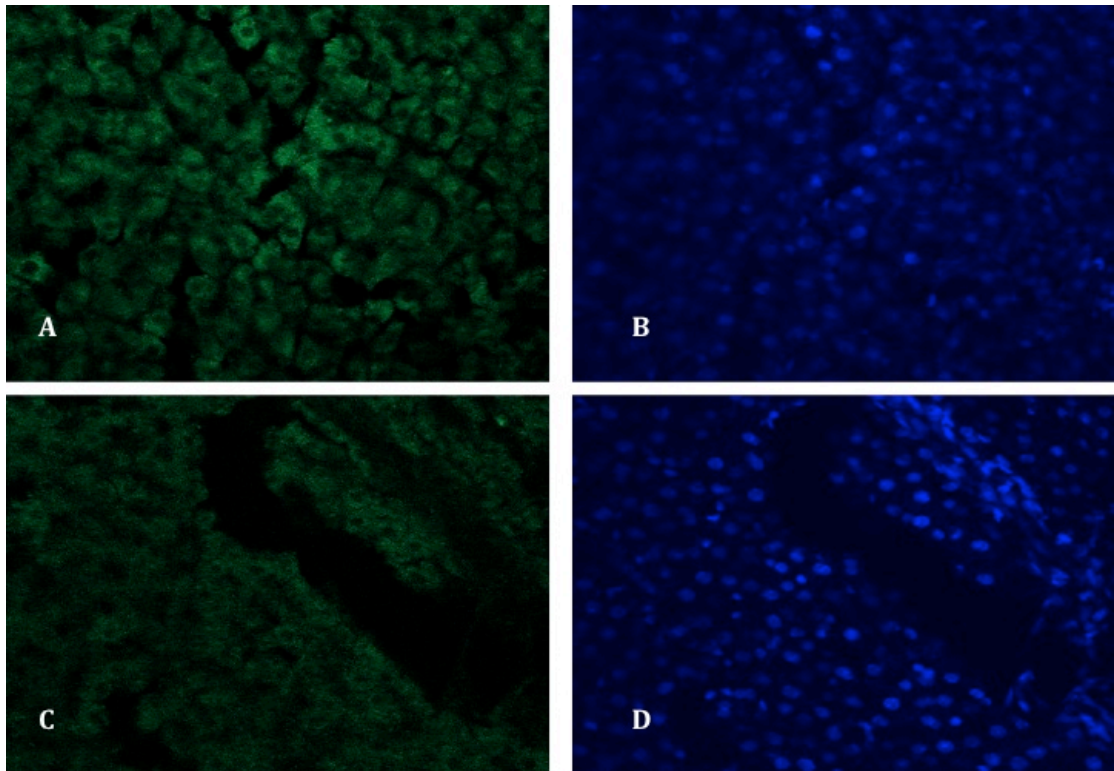
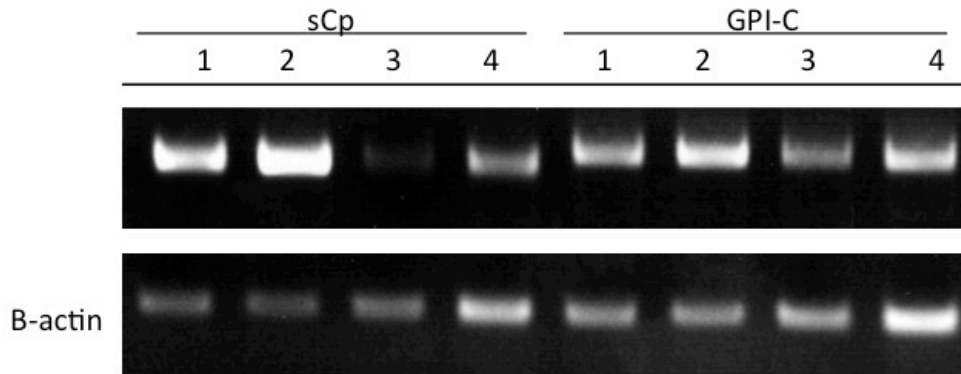


Figure 2

**A**



**B**

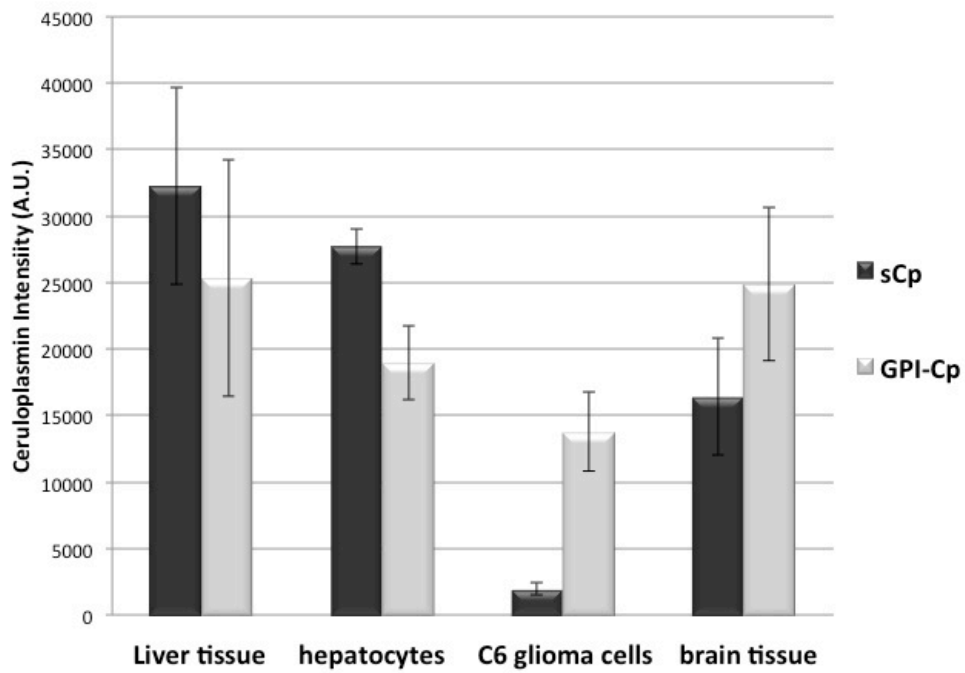


Figure 3

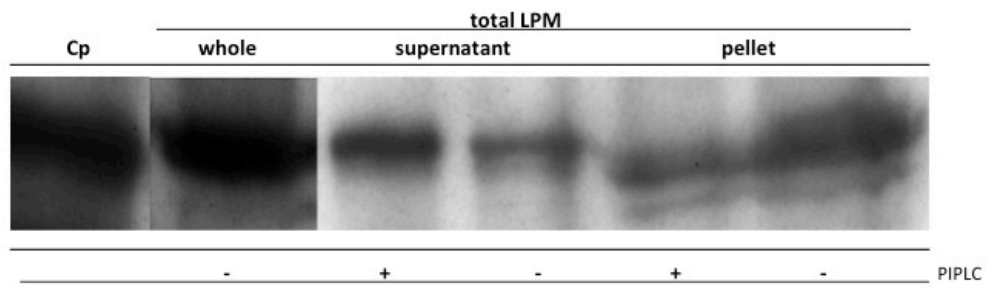
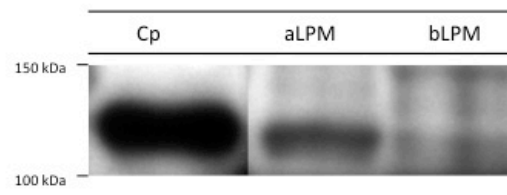


Figure 4

**A**



**B**

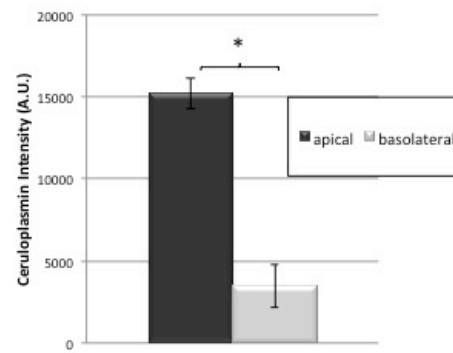


Figure 5

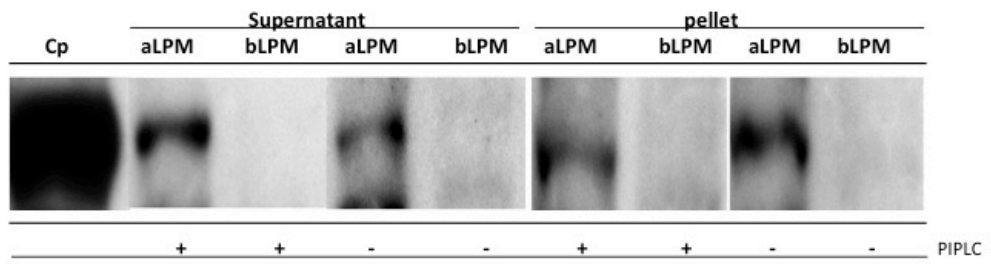


Figure 6

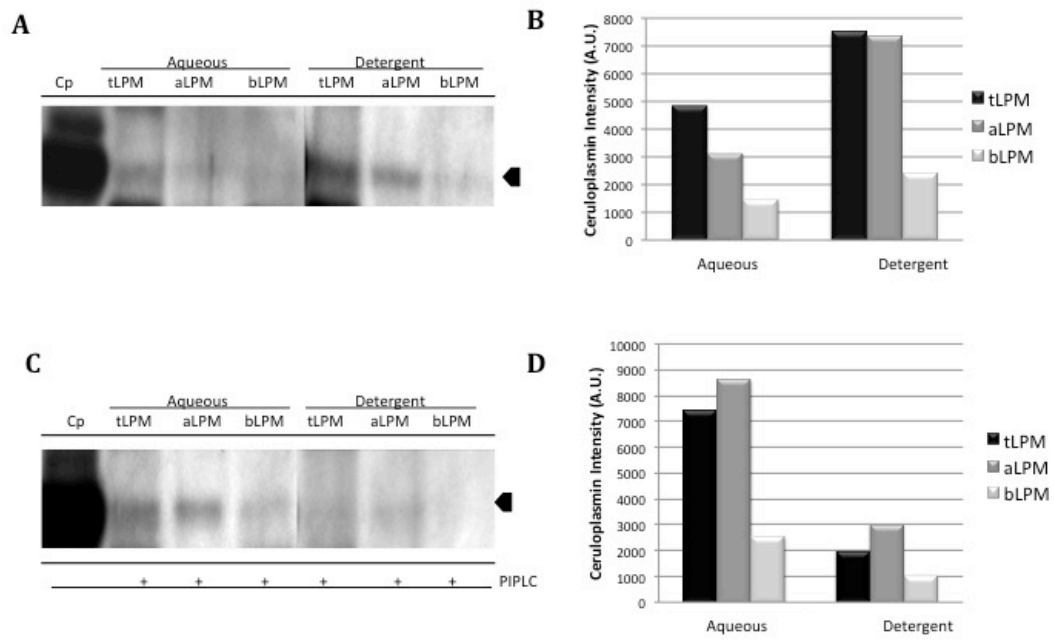




Figure 7

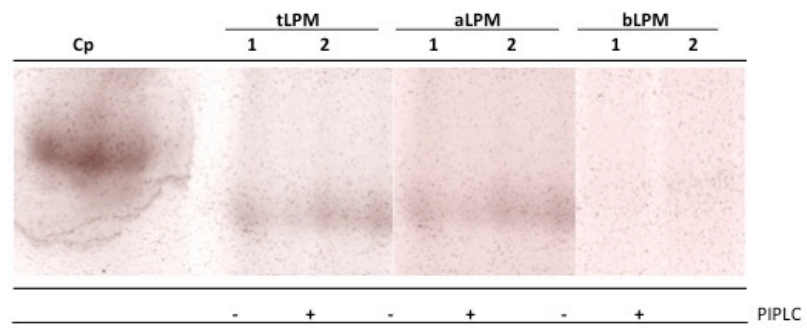


Figure 8

